

# Fabrication of SWNT/Silica Composites by the Sol–Gel Process

Keshwaree Babooram and Ravin Narain\*

Department of Chemistry and Biochemistry, Laurentian University, 935 Ramsey Lake Road, Sudbury, Ontario P3E 2C6, Canada

**ABSTRACT** Single-walled carbon nanotubes (SWNTs) have successfully been incorporated into a silica matrix using the sol–gel process. The SWNTs were first functionalized with 3-aminopropyltriethoxysilane (APTES) through an amide linkage formed between the carboxylic acid groups already present on their surface and the amino group on APTES. The silane moieties were then used to form silica with and without the presence of tetramethylorthosilicate (TMOS) in a sol–gel reaction. The addition of TMOS was found to influence the molecular arrangement of the SWNT in the silica matrix and also to retard the degradation of the silica–SWNT composite.

**KEYWORDS:** sol–gel • functionalization of carbon nanotubes • carbon nanotube–silica composites

## 1. INTRODUCTION

Silica compounds are among the most extensively studied materials, especially those prepared by the sol–gel process (1–3). However, their high brittleness and low resistance to mechanical stress tend to severely limit their scope of applications (4, 5). One possible and efficient way of improving the mechanical properties of silica materials is to reinforce them with fillers such as graphite powder (6), polymers (7), and carbon nanotubes (CNTs) (8). Since their discovery in 1991 (9), carbon nanotubes (CNTs) have attracted a great deal of interest from scientists all around the world because of their unique properties, which include mechanical strength, chemical stability, and electronic conductivity (10–12). For these reasons, the incorporation of SWNTs into conventional functional materials in order to enhance the performance of the latter has recently become a subject of major interest (13–15). However, the achievement of better performance in the composites heavily relies on the successful incorporation of the SWNT in the material being investigated. The insolubility in solvents due to strong intertube van der Waals attractions and the chemical inertness of SWNT are well-known factors that hinder their uniform dispersion and incorporation in any matrix (10, 16). This problem can be overcome by the functionalization of the SWNT with groups that facilitate their incorporation into a material through covalent bonding. For example, the covalent decoration of multiwalled carbon nanotubes (MWNT) with silica nanoparticles has successfully been carried out by Bottini et al. (17) using a water-in-oil microemulsion approach to control the size of the silica nanobeads. The latter activated the MWNT with carboxylic groups, to which 3-aminopropyltriethoxysilane was then attached in order to introduce silicon–ethoxide groups that could further be

hydrolyzed and condensed into silica using a sol–gel strategy. On the other hand, the reinforcement of silica with SWNT through covalent functionalization using 3-glycidoxypentyltrimethoxysilane (GPTMS) has been realized for the first time by Niu and co-workers (8). They have demonstrated improved mechanical properties and higher electron-transfer kinetics in the silica–SWNT composites as compared to pure silica.

In this research work, we aim at incorporating SWNT into silica through the covalent functionalization of the nanotubes using 3-aminopropyltriethoxysilane (APTES). The use of silane-terminated compounds for the functionalization of the SWNT creates a simple and easy way of building a homogeneous silica–SWNT composite through sol–gel chemistry. Generally, the sol–gel process consists of polymerization reactions which are based on the hydrolysis and condensation of alkoxide groups (18). Briefly, in the first step of the reaction where a silane compound is used, the Si–alkoxide group is hydrolyzed by a water molecule. Once the hydrolysis step has been initiated, the next reaction that follows is condensation of the hydrolyzed molecules to produce Si–O–Si linkages or networks. Further condensation reactions can then take place, leading to the formation of longer chains or oligomers. Eventually, there is the formation of more extended networks in the sol through further polymerization of the chains and oligomers.

In this work, we have successfully prepared amide-functionalized SWNT (using 3-aminopropyltriethoxysilane (APTES)) which were then incorporated into a homogeneous silica matrix through a sol–gel process by the hydrolysis and condensation reactions of the silane groups on APTES. In a separate reaction, tetraethyl orthosilicate (TMOS) was added to the sol–gel step in order to enhance the formation of the silica network by helping in the cross-linking process. The effect of the addition of TMOS to the sol–gel reaction on the thermal stability of the silica–SWNT composites was studied by thermogravimetric analysis (TGA). The SWNT–APTES and silica–SWNT ma-

\* To whom correspondence should be addressed. E-mail: rnarain@laurentian.ca. Tel: 1 705 675 1151 (2186). Fax: 1 705 675 4844.  
Received for review October 16, 2008 and accepted December 5, 2008

DOI: 10.1021/am8001296

© 2009 American Chemical Society

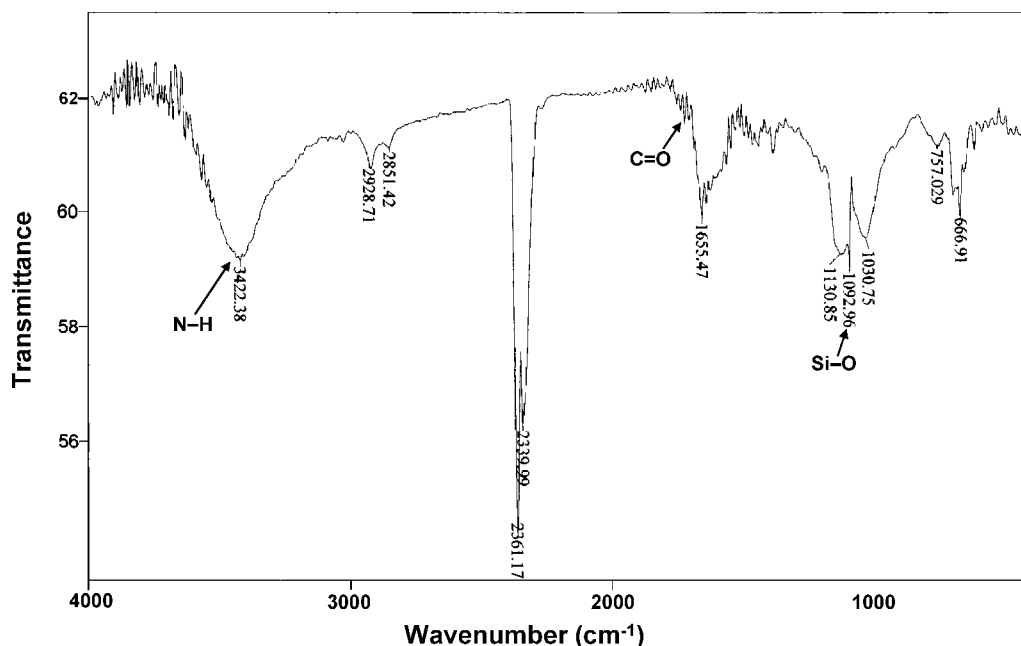
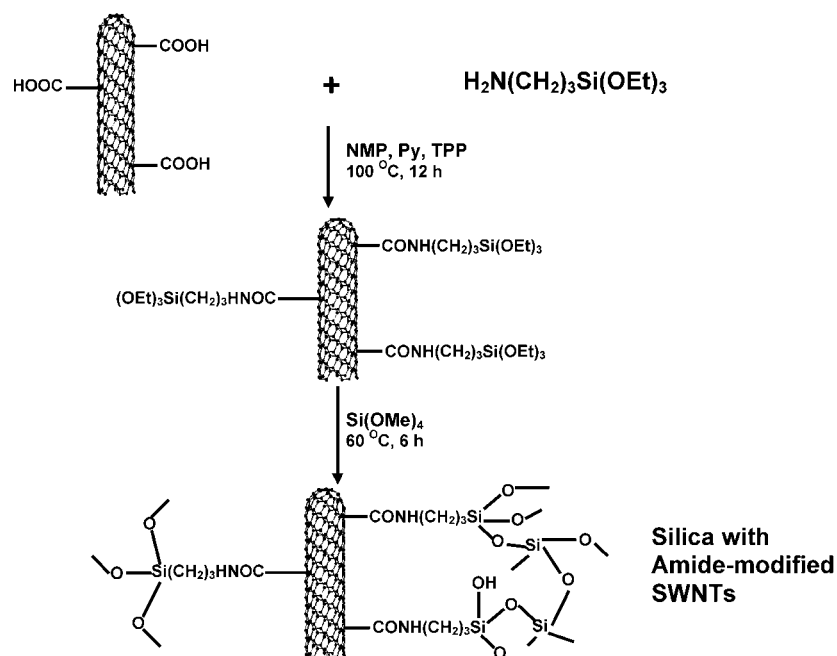


FIGURE 1. Infrared spectrum of the APTES-functionalized SWNT.

### Scheme 1. Synthesis of the Silica–SWNT Composites



materials were characterized by Raman spectroscopy to gain an insight of the change in structure after surface modification of the SWNT and their incorporation into silica. The morphology of these materials was also studied by scanning electron microscopy, which showed the homogeneous distribution of the nanotubes in the silica matrix.

## 2. EXPERIMENTAL SECTION

**2.1. Materials.** The carboxylic acid functionalized SWNTs (carboxylic acid content of 6 atom %) were purchased from Carbon Solutions Inc. 3-Aminopropyltriethoxysilane (APTES) and tetramethyl orthosilicate (TMOS) were purchased from Sigma-Aldrich. All the chemicals were used as received.

**2.2. Characterization.** Fourier transform infrared spectroscopy (FTIR) was carried out on a Bomem MB spectrometer to obtain structural information on the APTES-functionalized SWNT and silica–SWNT composites. Powder X-ray diffraction (XRD) using Cu K $\alpha$  radiation (40 Kv, 30 mA) was carried out on a Philips 1728 diffractometer in order to investigate any change in phase after the incorporation of the carbon nanotubes into a silica matrix. The morphology of the functionalized nanotubes and their silica composites was studied by scanning electron microscopy (SEM) using a Cameca SX-50 automated electron probe microanalyzer (OGL). Thermogravimetric analysis (TGA) was used to investigate the thermal stability of the silica–SWNT composite materials as well as to determine the silica content of the composites. The samples were analyzed on a SDT Q600 instrument. Raman spectra were measured on a LABRAM-HR

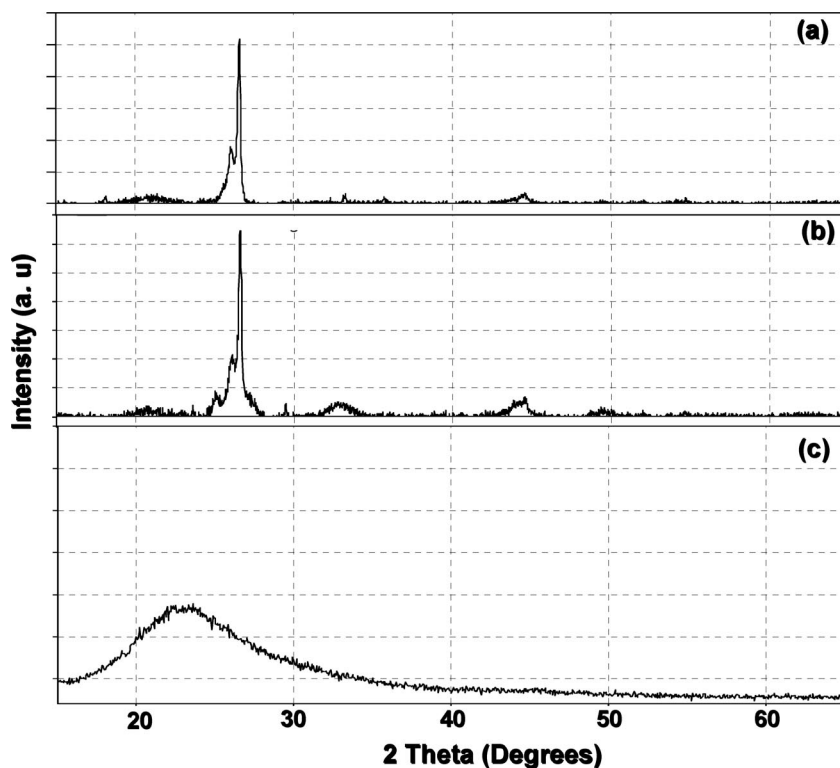


FIGURE 2. Powder X-ray diffraction (XRD) spectra of (a) the APTES-functionalized SWNT, (b) the SWNT-silica composite prepared without TMOS, and (c) the SWNT-silica composite prepared with TMOS.

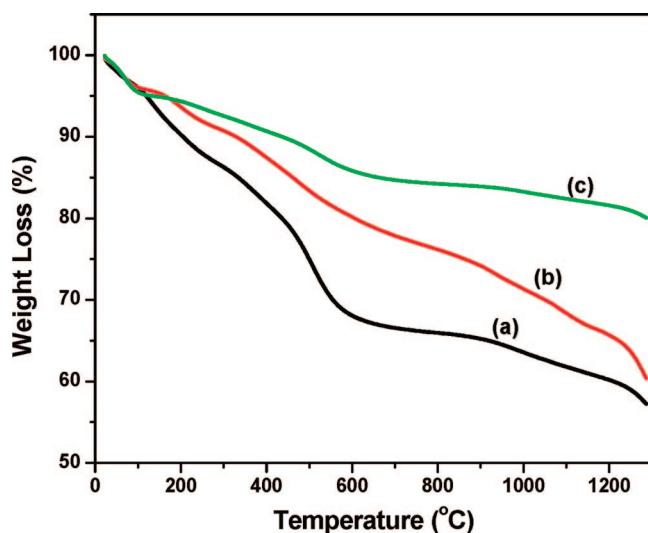


FIGURE 3. Thermogravimetric analyzes (TGA) measured from room temperature to 1300 °C under a nitrogen atmosphere of (a) the APTES-functionalized SWNT and the silica-SWNT composites prepared (b) without TMOS and (c) with TMOS.

confocal laser MicroRaman spectrometer with an argon ion laser at an excitation wavelength of 514.5 nm.

**2.3. Synthesis of Amide-Functionalized SWNTs.** Carboxylic acid functionalized SWNT (20 mg) was weighed into a round-bottom flask, *N,N'*-dimethylformamide (DMF, 15 mL), triphenylphosphine (TPP, 1 mg), and a few drops of pyridine were added, and the mixture was sonicated for 30 min. 3-Aminopropyltriethoxysilane (APTES; 4 mL, 17 mmol) was added slowly to the mixture with stirring, and the reaction was allowed to occur at 100 °C for 5 h for the formation of amide linkages between the carboxylic groups on the SWNTs and the amine group on the APTES. The black product (48 mg) was then

collected by suction filtration, and it was washed thoroughly with ethanol and dried under vacuum overnight.

**2.4. Synthesis of Silica-SWNT Composites.** Distilled water (15 mL) was added to the amide-functionalized SWNT (20 mg), and tetramethoxysilane (TMOS, 1 mL, 6.8 mmol) was then added slowly with stirring. The mixture was then heated at 60 °C for 6 h to allow the hydrolysis and condensation of the ethoxysilane groups on the amide-functionalized SWNT and TMOS. The product was removed from the reaction flask by suction filtration and washed several times with ethanol and then dried under vacuum overnight. In another reaction, the amide-functionalized SWNT was heated with water at 60 °C for 6 h in the absence of TMOS. The aim of this reaction was to build a silica network through the hydrolysis and condensation of ethoxysilane groups present on the amide-functionalized SWNT only. The procedure for the synthesis of the silica-SWNT composites from the carboxylic acid functionalized SWNT is illustrated in Scheme 1.

### 3. RESULTS AND DISCUSSION

#### 3.1. Synthesis of the Silica-SWNT Composites.

The first step toward the synthesis of the silica-SWNT composites was the functionalization of the SWNT-COOH species with APTES so that the terminal ethoxide groups from the latter are then available for hydrolysis and condensation in order to form a silica matrix in the final step. The reaction of the amine group on APTES with the carboxylic groups on the SWNT to form an amide linkage was confirmed by infrared spectroscopy. The IR spectrum of the APTES-functionalized SWNT is shown in Figure 1. The peaks at  $\sim 3422\text{ cm}^{-1}$  (for the N-H bond),  $\sim 1700\text{ cm}^{-1}$  (for the C=O group), and  $1092\text{ cm}^{-1}$  (for the Si-O bond) clearly indicate the covalent attachment of the APTES to the SWNT through an amide linkage. Similar IR spectra (not shown)

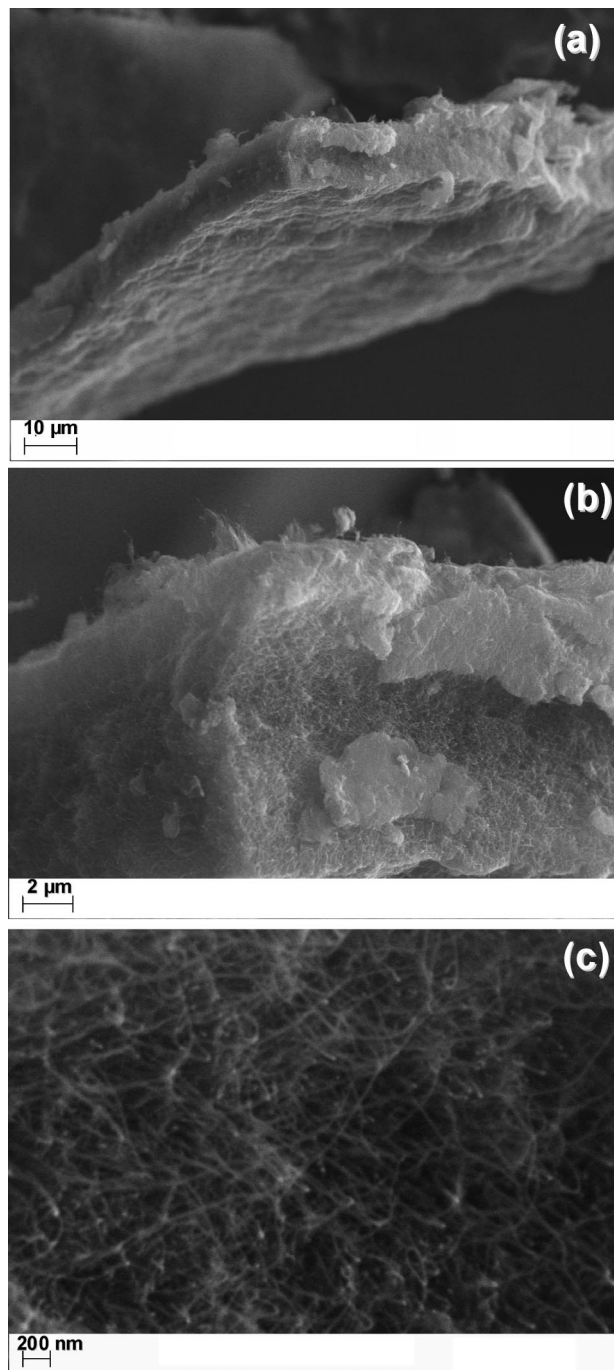


FIGURE 4. Scanning electron microscopic (SEM) images of the SWNT-silica composite synthesized without TMOS.

were obtained after the sol-gel reaction to obtain the silica-SWNT composites.

**3.2. X-ray Diffraction (XRD) of the APTES-Functionalized SWNT and Silica-SWNT Composites.** Powder X-ray diffraction (XRD) was performed on the APTES-functionalized nanotubes and the silica-SWNT composites in order to study the change in phase of the carbon nanotubes after incorporation into the silica. The XRD spectra of the functionalized SWNTs and their silica composites are shown in Figure 2. The intense crystalline peak seen on the XRD pattern of the APTES-functionalized SWNTs (Figure 2a) at a  $2\theta$  value of  $\sim 26.7^\circ$  is characteristic of the carbon

nanotubes. After the formation of the silica matrix using only the silicon-alkoxy groups present on the nanotubes' surface, broadening of this peak is observed (Figure 2b), showing the successful formation of the silica matrix. This shows that this silica-SWNT composite is semicrystalline in nature. In contrast, the silica-SWNT composite that was formed with the addition of TMOS to the sol-gel reaction showed a completely amorphous character (Figure 2c). This is due to the presence of a composite material, the bulk of which is mostly composed of silica.

**3.3. Thermogravimetric Analysis (TGA) of the Silica-SWNT Composites.** The thermal behavior of the APTES-functionalized SWNT and the silica-SWNT composites were studied by thermogravimetric analysis (TGA). All the samples were heated under a nitrogen atmosphere from room temperature to 1300 °C at a heating rate of 20 °C/min. The TGA curves of the APTES-functionalized SWNT and the silica-SWNT composites synthesized with and without TMOS in the sol-gel step are displayed in Figure 3. The TGA curve of the APTES-functionalized SWNT (curve a) shows two weight losses around 300 and 400 °C, respectively, corresponding to the decomposition of the organic groups attached to the surface of the SWNT. After the incorporation of the functionalized SWNT into the silica matrix, an increase in the thermal stability of the composites can clearly be seen in Figure 3 by an increase in the decomposition temperature to around 500 °C. The thermal degradation of the composite materials is also seen to slow down by the addition of TMOS to the sol-gel step for the formation of the silica-SWNT. The change in the decomposition patterns of the silica-SWNT composites relative to that of the APTES-functionalized SWNT confirms the formation of the silica matrix in both composite materials. An increase in the residual weights (corresponding to residual carbon and silica) of the materials analyzed is also observed from 57% in the APTES-functionalized SWNT to 60% (curve b) and 80% (curve c) in the silica-SWNT prepared without and with TMOS, respectively. The results are consistent with the fact that the silica content of the APTES-functionalized SWNT does not differ by much from that of the silica-SWNT synthesized without the addition of TMOS, because the latter was formed by the hydrolysis and condensation of the silicon-ethoxide groups present on the APTES-functionalized SWNT only.

**3.4. Scanning Electron Microscopic Analysis of the Silica-SWNT Composites.** The silica-SWNT composites were imaged using scanning electron microscopy (SEM), which revealed some very interesting features about their microstructure and morphology. The SEM pictures of the composites are shown in Figures 4 and 5, respectively. Figure 4a depicts the cross-section of a slab of the silica-SWNT composite prepared without the addition of TMOS to the sol-gel step. These pictures clearly show the homogeneous dispersion of the carbon nanotubes in a closely packed silica matrix. Parts b and c of Figure 4 are pictures of the same slab taken at higher magnification to show how the functionalized SWNTs have successfully been cross-linked to

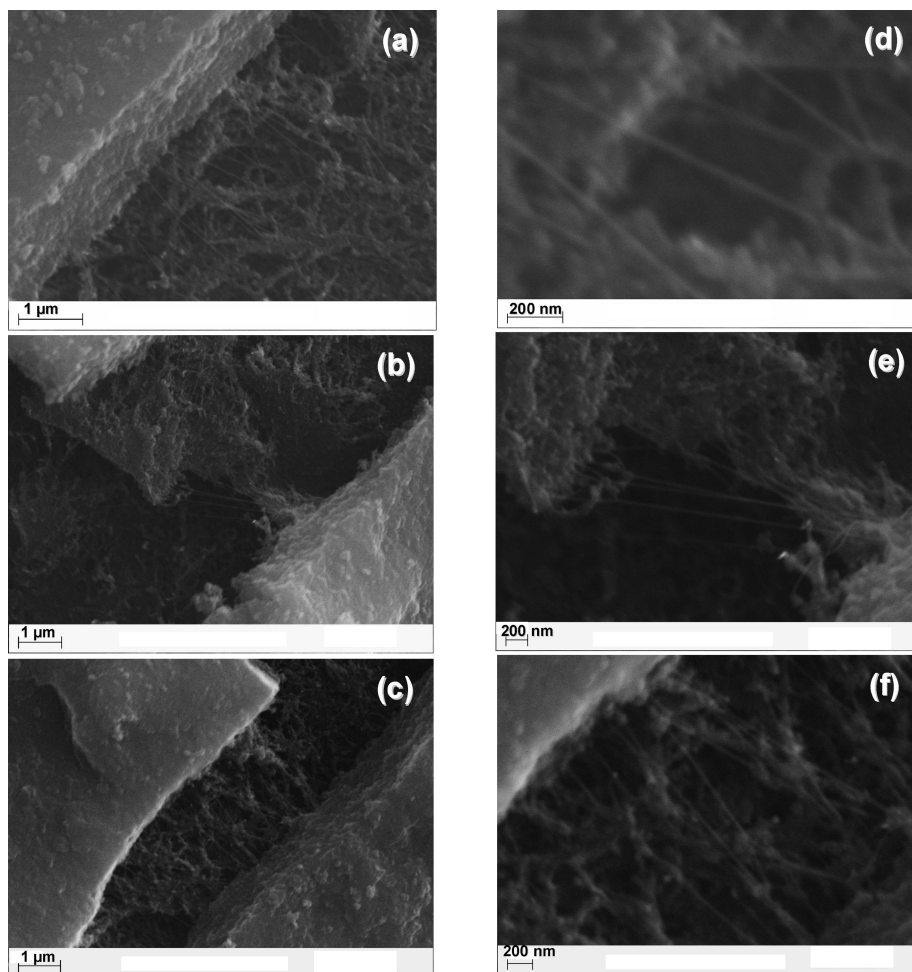


FIGURE 5. Scanning electron microscopic (SEM) images of the SWNT-silica composite prepared by the addition of TMOS to the sol-gel step.

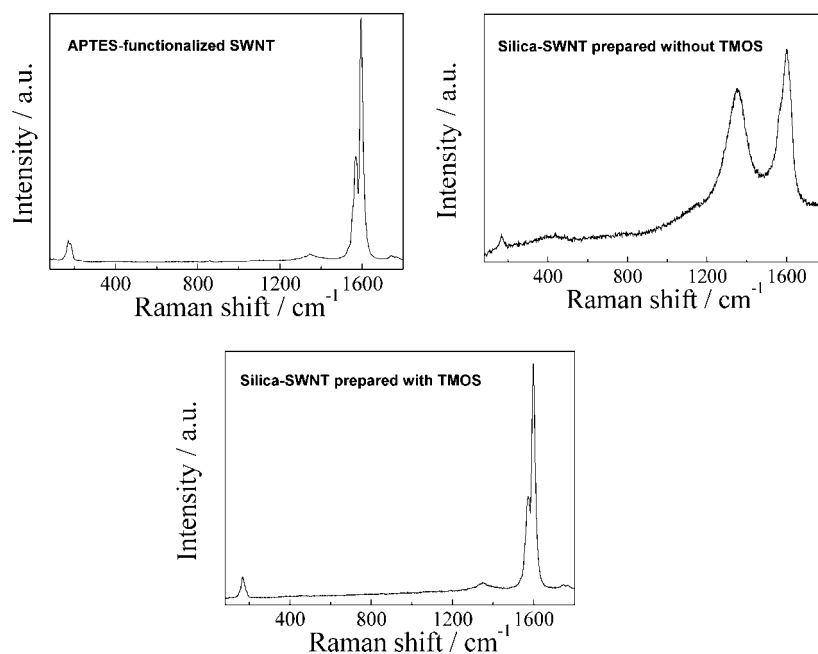


FIGURE 6. Raman spectra of the APTES-functionalized SWNT and the silica-SWNT composites.

each other through the silica, forming a network in which the nanotubes are intertwined. This is in good agreement

with the speculation that the silicon-ethoxide groups attached to the nanotubes' surface through the APTES mol-

ecule have been hydrolyzed in the sol–gel reaction and have subsequently randomly condensed with other similar groups, hence cross-linking together the carbon nanotubes into an intertwined network.

On the other hand, a completely different scenario is seen in Figure 5, in the SEM micrographs of the silica–SWNT composite synthesized in the presence of TMOS. It can be concluded that this composite was formed as a layered material with a thick and compact silica layer on top of the silica–SWNT layer (Figure 5a–c). As a crack was formed in the first layer (most probably during the drying process and because of the high brittleness of pure silica), we can observe the SWNTs embedded in a silica matrix. Interestingly, the nanotubes appear to stretch out in one direction, looking as if they were being pulled upon when the layers cracked (Figure 5d–f). While the upper layer consisting of pure silica cracked very easily, the one which contains the SWNTs showed resistance to breakage. This shows the ability of the nanotubes to impart their mechanical strength to the silica.

**3.5. Raman Spectroscopic Data of the Silica–SWNT Composites.** Raman spectroscopy is a widely used technique for the characterization of SWNT in order to gain useful information about their structure. Figure 6 shows the Raman spectra of the APTES-functionalized SWNT and the silica–SWNT composites. The band observed at  $\sim 1350\text{ cm}^{-1}$  (referred to as the D band) represents disordered  $\text{sp}^3$  carbon structure, and the band at  $\sim 1600\text{ cm}^{-1}$  (G band) results from  $\text{sp}^2$  ordered crystalline graphite-like structures (10, 19). For the silica–SWNT composites prepared without TMOS, an increase of the D band is observed together with a broadening of both the D and G bands. This observation is indicative of an increase in defect due to covalent attachment to the nanotubes and also due to the strain put on their surfaces as a result of the cross-linking between the nanotubes. This kind of arrangement brings the carbon nanotubes closer together which, therefore, influences the molecular band structure. These results agree very well with the observation made in the SEM pictures of this silica–SWNT composite (see section 3.4) where the SWNTs are intertwined and closely packed in the silica matrix. However, when TMOS was used in the cross-linking process of the functionalized SWNTs, only a small intensity increase and a small enhancement of the bands was observed. This can be explained by the fact that the addition of the TMOS resulted in the formation of a composite with a higher silica content that tends to mask the effect from the carbon nanotubes. The TMOS also serves as a medium of cross-linking between the carbon nanotubes, which tends to ease off the strain from the nanotubes' surface.

#### 4. CONCLUSIONS

Amide-functionalized SWNTs were prepared by the reaction of SWNT–COOH with APTES. The APTES-functionalized SWNTs were then incorporated into a silica matrix using sol–gel chemistry. In the first case, the silica network was formed simply through the hydrolysis and condensation of the silane groups present on the APTES attached to the walls

of the SWNT. In another reaction, TMOS was added to the sol–gel step to help form the silica matrix. IR spectroscopy was used to confirm the formation of the amide bond between the SWNT–COOH and APTES as well as the formation of the silica network in the composites synthesized with and without TMOS. The successful incorporation of the SWNTs into a silica matrix has been confirmed by both XRD and SEM analyses. The latter has shown a homogeneous distribution of intertwined nanotubes in a compact silica matrix in the composite formed without TMOS. The thermal stability of the APTES-functionalized SWNT was compared to those of the silica–SWNT composites. The incorporation of the SWNT into a silica network was shown to retard the thermal degradation of the composite materials. Raman studies have shown that, in the absence of TMOS, the molecular band structure of the resulting silica–SWNT composite is greatly disrupted because of extra strain on the nanotubes due to the cross-linking between the nanotubes. Through the successful incorporation of an amide-functionalized SWNT into silica, we have prepared composites that are less brittle compared to pure silica and that can also have potential applications as fillers in the reinforcement of high-performance polymers such as polyamides, polyimides, polycarbonates, and polyether ether ketone (PEEK) polymers.

**Acknowledgment.** We thank the Ontario Centre of Excellence, Materials and Manufacturing Ontario, for financial support of this research. Prof. Shiyong Liu, Department of Polymer Science and Engineering, University of Science and Technology of China, Hefei, People's Republic of China, is acknowledged for his assistance in obtaining the Raman spectra.

#### REFERENCES AND NOTES

- (1) Hench, L. L.; West, J. K. *Chem. Rev.* **1990**, *90*, 33–72.
- (2) Sakka, S., Ed. *Handbook of Sol-gel Science and Technology: Processing, Characterization and Applications*; Kluwer: Dordrecht, The Netherlands, 2005.
- (3) Husing, N.; Schubert, U. *Angew. Chem., Int. Ed.* **1998**, *37*, 22–45.
- (4) Gill, I. *Chem. Mater.* **2001**, *13*, 3404–3421.
- (5) Yang, H.; Shi, Q.; Tian, B.; Xie, S.; Zhang, F.; Yan, Y.; Tu, B.; Zhao, D. *Chem. Mater.* **2003**, *15*, 536–541.
- (6) Tsionsky, M.; Gun, G.; Glezer, V.; Lev, O. *Anal. Chem.* **1994**, *66*, 1747–1753.
- (7) Wang, B. Q.; Li, B.; Wang, Z. X.; Xu, G. B.; Wang, Q.; Dong, S. J. *Anal. Chem.* **1999**, *71*, 1935–1939.
- (8) Zhang, Y.; Shen, Y.; Han, D.; Wang, Z.; Song, J.; Niu, L. *J. Mater. Chem.* **2006**, *16*, 4592–4597.
- (9) Iijima, S. *Nature* **1991**, *354*, 56.
- (10) Haddon, R. C. *Acc. Chem. Res.* **2002**, *35*, 997–1113.
- (11) Ajayan, P. M. *Chem. Rev.* **1999**, *99*, 1787–1799.
- (12) Bianco, A.; Prato, M. *Adv. Mater.* **2003**, *15*, 1765–1768.
- (13) Huang, J. E.; Li, X.-H.; Xu, J.-C.; Li, H.-L. *Carbon* **2003**, *41*, 2731–2736.
- (14) Curtin, W. A.; Sheldon, B. W. *Mater. Today* **2004**, *7* (11), 44–49.
- (15) Wagner, H. D.; Vaia, R. A. *Mater. Today* **2004**, *7* (11), 38–42.
- (16) Bower, C.; Rosen, R.; Zhou, O. *Appl. Phys. Lett.* **1999**, *74*, 3317–3319.
- (17) Bottini, M.; Tautz, L.; Huynh, H.; Monosov, E.; Bottini, N.; Dawson, M. I.; Bellucci, S.; Mustelin, T. *Chem. Commun.* **2005**, 758–760.
- (18) Bradley, D. C. *Chem. Rev.* **1989**, *89*, 1317–22.
- (19) Zhang, Y.; Shen, Y.; Li, J.; Niu, L.; Dong, S.; Ivaska, A. *Langmuir* **2005**, *21*, 4797–4800.

AM8001296